A continuous reaction network that produces RNA precursors

Ruiqin Yi[a], Quoc Phuong Tran[b], Sarfaraz Ali[b], Isao Yoda[c], Zachary R. Adam[d,e], H. James Cleaves II[a,e,f], and Albert C. Fahrenbach[b,1]

[a]Earth-Life Science Institute, Tokyo Institute of Technology, Tokyo 152-8550, Japan; [b]School of Chemistry, University of New South Wales, Sydney, NSW 2052, Australia; [c]Co-60 Radiation Facility, Tokyo Institute of Technology, Tokyo 152-8550, Japan; [d]Department of Planetary Sciences, University of Arizona, Tucson, AZ 85721; [e]Blue Marble Space Institute of Science, Seattle, WA 98154; and [f]Program in Interdisciplinary Studies, Institute for Advanced Study, Princeton, NJ 08540

Edited by Chad A. Mirkin, Northwestern University, Evanston, IL, and approved April 17, 2020 (received for review December 19, 2019)

Continuous reaction networks, which do not rely on purification or timely additions of reagents, serve as models for chemical evolution and have been demonstrated for compounds thought to have played important roles for the origins of life such as amino acids, hydroxy acids, and sugars. Step-by-step chemical protocols for ribonucleotide synthesis are known, but demonstrating their synthesis in the context of continuous reaction networks remains a major challenge. Herein, compounds proposed to be important for prebiotic RNA synthesis, including glycolaldehyde, cyanamide, 2-aminooxazole, and 2-aminoimidazole, are generated from a continuous reaction network, starting from an aqueous mixture of NaCl, NH_4Cl, phosphate, and HCN as the only carbon source. No well-timed addition of any other reagents is required. The reaction network is driven by a combination of γ radiolysis and dry-down. γ Radiolysis results in a complex mixture of organics, including the glycolaldehyde-derived glyceronitrile and cyanamide. This mixture is then dried down, generating free glycolaldehyde that then reacts with cyanamide/NH_3 to furnish a combination of 2-aminooxazole and 2-aminoimidazole. This continuous reaction network models how precursors for generating RNA and other classes of compounds may arise spontaneously from a complex mixture that originates from simple reagents.

systems chemistry | radiolysis | prebiotic chemistry | RNA world | wet–dry cycles

The complex and far-from-equilibrium nature of biochemical reaction networks may have originated from simpler nonliving ones (1, 2), which nevertheless may have contained a large number of interacting organic compounds. A variety of reaction networks capable of generating complex mixtures of molecules hypothesized to be relevant to life's origins have been demonstrated, particularly for amino acids (3, 4), hydroxy acids (5), and sugars (6–8). The RNA world hypothesis (9) has led to the investigation of possible prebiotic synthetic pathways for RNA, in particular the ribonucleoside monophosphates (10–16). Critiques (6, 17–20) of these pathways, however, have focused on the fact that many of the experimental procedures employ step-by-step chemical protocols or well-timed addition steps, which are suggested to be implausible in environmental settings. These types of procedures have previously been referred to as "discontinuous synthesis" models (19), with experimental interventions conducted to minimize the production of complex mixtures in favor of specific targets. Although investigations of stepwise syntheses are crucial for reaction pathway discovery, it is still unclear whether such chemical protocols can be realized in the context of hypothetical continuous reaction networks from which early life may have emerged.

Here, a "continuous reaction network" is defined as one which is minimally manipulated (21), to most accurately simulate a natural environment, e.g., in which intermediates are not purified, side products are not removed, and new reagents other than the initial starting materials are not added. Therefore, the synthesis of target molecules must occur in the presence of whatever side products also formed as a consequence of the initial conditions. The basic feedstocks of prebiotic chemistry are thought to be small molecules of a limited type, i.e., C1 compounds (22). Thus, the reaction network ought to begin with a set of small molecules that are likely to have been provided by the environment. The aim of this study is not an attempt to prove a specific geological scenario, but to assess whether continuous reaction networks are capable of producing RNA precursors, and ultimately RNA itself.

Herein, a continuous reaction network that generates RNA precursors according to the constraints described above is demonstrated. This reaction network begins with hydrogen cyanide (HCN) as the only organic feedstock, along with sodium chloride (NaCl), ammonium chloride (NH_4Cl), and inorganic phosphate (P_i). HCN is a common chemical product of an array of high-energy atmospheric processes, for example, UV radiation-driven photochemistry, fixation by lightning, atmospheric impingement of energetic particles, and impact-induced aerodynamic ablation (23, 24). This mixture is then made to react by exposure to ionizing gamma (γ) radiation. After dry-down of the resulting mixture, compounds known to be important for abiotic RNA synthesis, in particular, cyanamide, glycolaldehyde, 2-aminooxazole, and 2-aminoimidazole are produced.

2-Aminooxazole and 2-Aminoimidazole Synthesis in the Context of the RNA World Hypothesis

One of the most well-studied abiotic syntheses of the pyrimidine ribonucleotides, employing simple reagents and conditions, was

Significance

RNA may have been the original polymer to arise spontaneously on the early Earth through natural geochemistry. Although direct physical evidence regarding early Earth's geochemistry is extremely limited, complex chemical reaction networks are thought to have played an important role in chemical evolution. The present study demonstrates an experimental model reaction network that generates a number of compounds that can lead to RNA synthesis in a single mixture starting from simple organic and inorganic feedstocks. Models of this type will help explain which conditions are needed to produce RNA in primitive planetary settings.

Author contributions: R.Y., Z.R.A., H.J.C., and A.C.F. designed research; R.Y., Q.P.T., S.A., I.Y., and A.C.F. performed research; R.Y., Q.P.T., S.A., and A.C.F. analyzed data; and R.Y., Z.R.A., H.J.C., and A.C.F. wrote the paper.

The authors declare no competing interest.

This article is a PNAS Direct Submission.

Published under the PNAS license.

[1]To whom correspondence may be addressed. Email: a.fahrenbach@unsw.edu.au.

This article contains supporting information online at https://www.pnas.org/lookup/suppl/doi:10.1073/pnas.1922139117/-/DCSupplemental.

First published June 2, 2020.

CHEMISTRY

pioneered by Orgel and coworkers (10) and extensively elaborated by Sutherland and coworkers (11, 25). Instead of direct condensation of ribose with a pyrimidine, both the D-ribose and nucleobase components are built up concurrently. This synthesis, sometimes referred to as the Powner–Sutherland pathway, makes use of simple hydroxyaldehydes, namely, glycolaldehyde and D-glyceraldehyde (Scheme 1). The first step is the reaction of glycolaldehyde with cyanamide in the presence of P_i, which acts as a general-base catalyst, yielding 2-aminooxazole. This compound can serve as an intermediate for both cytidine and uridine 2′,3′-cyclic phosphates. Szostak and coworkers (26) later demonstrated that when NH_4Cl is added to the mixture of glycolaldehyde and cyanamide, 2-aminoimidazole is produced (see refs. 11 and 26 for discussion of the proposed mechanisms), a structurally similar compound that serves as an effective leaving group in the context of nonenzymatic template-directed RNA synthesis (27). 2-Aminooxazole selectively reacts with glyceraldehyde, potentially allowing 2-aminoimidazole to accumulate for later use. Although flow chemistry has been employed to synthesize 2-aminooxazole without purification (28), orderly mixing of reagents was still required. A reaction network that generates both 2-aminooxazole and 2-aminoimidazole from a common carbon source and in a continuous fashion has yet to be demonstrated (29).

Radiolysis as a Driving Force

Chemical evolution (30) requires energy. Radiolysis from ionizing radiation (31–33) as well as UV-photolysis (34) are often employed in order to model early Earth aqueous chemistry. Both sources of energy have been shown capable of generating solvated electrons (e^-_{aq}) in aqueous environments, and in the case of γ rays, ionization of water is what leads to e^-_{aq} in addition to hydroxyl radical (·OH) and hydrogen atom (·H) production. The generation of e^-_{aq} in the presence of excess HCN has been shown to lead to simple sugars (35–37). This reaction works by a Kiliani–Fischer homologation mechanism, whereby e^-_{aq} effectively serves as the reducing agent. This mechanism is an alternative to the often-cited formose reaction (6–8) as a source of simple sugars for forming nucleotides. In the first step (Scheme 2), HCN is reduced to methanimine, which hydrolyzes to formaldehyde. Next, formaldehyde reacts with another molecule of HCN to yield glycolonitrile **1**. Reduction of the nitrile followed by hydrolysis of the resulting imine generates glycolaldehyde. In the presence of excess HCN, glycolaldehyde equilibrates to its cyanohydrin, glyceronitrile **2**, which has the potential to be reduced further to glyceraldehyde. γ Radiolysis of dilute HCN with molar concentrations of NaCl and NH_4Cl salts produces (35) not only the glycolaldehyde-derived glyceronitrile, but also cyanamide as major components among a complex mixture of products. The production of cyanamide relies on the oxidizing power achieved through the radiolysis of briny water, in a mechanism that likely depends (35) on chlorine radical (Cl·) generation (for

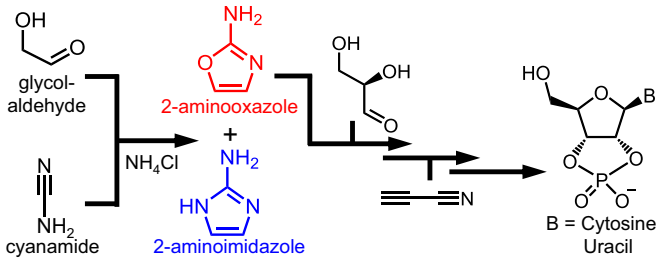

Scheme 1. Reaction pathway for the synthesis of 2-aminooxazole (11) and 2-aminoimidazole (26). The former is an intermediate in the Powner–Sutherland pathway for cytidine and uridine 2′,3′-cyclic phosphates, and the latter an effective leaving group for nonenzymatic template-directed RNA synthesis.

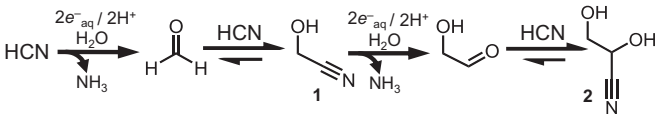

Scheme 2. The Kiliani–Fischer synthesis of glycolaldehyde, which equilibrates to glyceronitrile given excess HCN. This version of the synthesis makes use of solvated electrons (e^-_{aq}) as the reducing agent.

more details, see ref. 35 and *SI Appendix*, Schemes). High concentrations of NaCl favor cyanamide through a pathway that may involve cyanogen chloride as an intermediate, a compound which was also observed (Scheme 3). Cyanogen chloride itself is proposed to form by reaction of $^-$CN with radiolytically produced HOCl, although another pathway could involve a Cl-containing radical intermediate. This radiolytic reaction network has the potential to produce 2-aminooxazole and 2-aminoimidazole starting from simple initial conditions in a continuous manner, if glyceronitrile can be employed as a source of glycolaldehyde in the synthesis.

Results

Dry-Down Enables 2-Aminooxazole Synthesis. The first step in the synthesis of 2-aminooxazole is nucleophilic addition of cyanamide to the carbonyl of glycolaldehyde (Scheme 4, *Top*). Excess cyanide almost completely inhibits the reaction (Scheme 4, *Bottom*, and *SI Appendix*, Fig. S11) by forming glyceronitrile. Therefore, in order to form 2-aminooxazole efficiently, the cyanide anion must first be removed or suppressed. It was hypothesized that removal of excess HCN by evaporation would shift the cyanohydrin equilibrium by Le Chatelier's principle away from glyceronitrile toward free glycolaldehyde, enabling the synthesis of 2-aminooxazole. In order to test this supposition, cyanamide and glycolaldehyde were combined with excess NaCN in phosphate buffer (Fig. 1*A*). The ^{1}H NMR spectrum of this mixture (Fig. 1*B*) shows a doublet at 3.85 ppm assigned to the C2 protons of glyceronitrile, while almost no free glycolaldehyde (predominantly present in the gem-diol form) was detected. The mixture was then dried under reduced pressure and redissolved in 10% D_2O. A new doublet assigned to the C2 proton of glycolaldehyde appeared in the ^{1}H NMR spectrum. Heating at 50 °C resulted in two new resonances in the aromatic region assigned to 2-aminooxazole, while the signal for glycolaldehyde decreased proportionally. When the concentration of 2-aminooxazole started to plateau (Fig. 1*C*), another dry–wet cycle was carried out. Immediately after, the resonance of glycolaldehyde was observed to increase in intensity, although a decrease in the 2-aminooxazole concentration was also observed. The decreased 2-aminooxazole concentration may be a result of sublimation (38) during dry-down. Heating the solution once again resulted in further increase in the signals for 2-aminooxazole. A third dry–wet cycle (Fig. 1*C*) yielded still more 2-aminooxazole. These results confirm dry-down as an effective process for removing excess HCN, freeing up glycolaldehyde, and fostering the synthesis of 2-aminooxazole, affording its accumulation by repetitive cycling.

γ Radiolysis Combined with Dry-Down Enables 2-Aminooxazole and 2-Aminoimidazole Production. It was expected that an irradiated solution initially containing dilute (25 mM) HCN in the presence

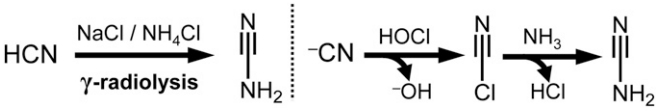

Scheme 3. Radiolysis of HCN with NaCl and NH_4Cl generates cyanamide (*Left*). A possible pathway involving cyanogen chloride is summarized on the *Right*.

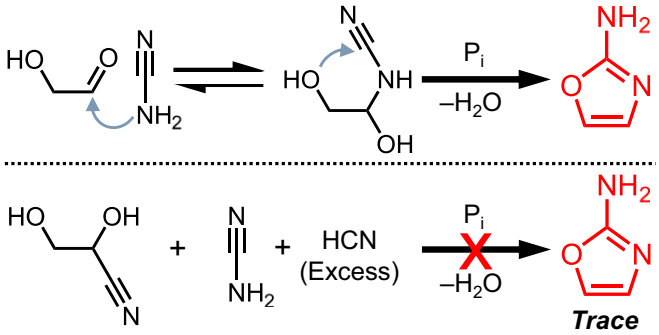

Scheme 4. Partial mechanism for 2-aminooxazole synthesis. The first step is addition of cyanamide to the carbonyl of glycolaldehyde (*Top*). In the presence of excess HCN, the glycolaldehyde-derived glyceronitrile forms and inhibits the reaction (*Bottom*).

of P_i and high concentrations of NH_4Cl and NaCl would also yield 2-aminooxazole following dry-down. Such a solution was subjected to γ irradiation for ∼1 d at pH 7 (Fig. 2*A*). The ^{1}H NMR spectrum was recorded (*SI Appendix*, Fig. S17), revealing a doublet at 3.85 ppm assigned to glyceronitrile (0.10 mM, 1.2%) and no free glycolaldehyde was detected. Large NaCl concentrations did not hinder the reduction pathways involved in the radiolytic production of glyceronitrile (*SI Appendix*, Fig. S12). Large NH_4Cl concentrations also permit these pathways (*SI Appendix*, Fig. S13). The cyanamide concentration in this irradiated solution was determined to be ∼0.65 mM, representing a 2.6% yield based on the initial cyanide content (*SI Appendix*, Fig. S8). Neutral pH was also found to favor the production of cyanamide and glyceronitrile during radiolysis (*SI Appendix*, Fig. S15). Although the cyanohydrins glycolonitrile and glyceronitrile are not stable under prolonged irradiation, cyanamide was (*SI Appendix*, Fig. S16), suggesting the possibility of long-term accumulation even under highly radioactive environments. Additional resonances were observed for a variety of other compounds that are discussed later.

The irradiated solution was then concentrated by ∼10-fold under reduced pressure. The cyanamide concentration was found to be 2.8 mM (*SI Appendix*, Fig. S9), which is approximately a factor of 2 away from the theoretical upper limit of 6.5 mM. The dry-down process resulted in the precipitation of a large amount NaCl, which is suspected to include smaller quantities of other inorganic and organic species, for example, cyanamide. Alternatively, the dry-down process itself may have resulted in its partial degradation. A sample of the homogeneous solution, i.e., without any solid precipitates, was removed and adjusted to pH 8, which previous studies have shown favor the synthesis of 2-aminooxazole (26). Samples kept at pH 7 were also investigated. The ^{1}H NMR spectrum (Fig. 2*B*, *Bottom* trace, and *SI Appendix*, Fig. S18) reveals a new doublet assigned to glycolaldehyde gem-diol. The concentration of glycolaldehyde was determined to be ∼0.16 mM,

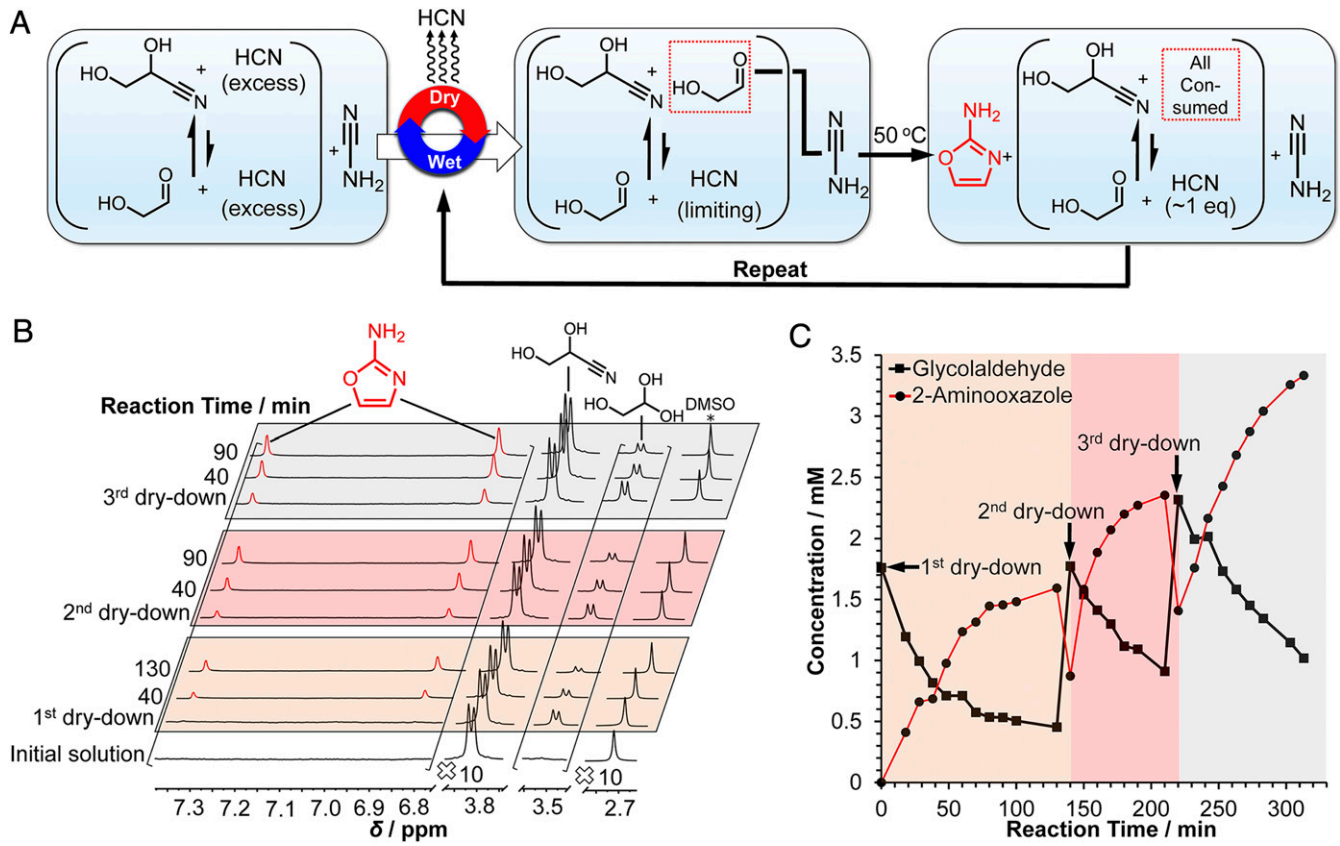

Fig. 1. (*A*) Scheme for the synthesis of 2-aminooxazole from repeated dry-down cycles starting from a solution containing cyanamide, glyceronitrile, NaCN, and P_i. (*B*) NMR analysis of the dry-down reaction depicted in *A*. A 500-μL solution of 0.1 M cyanamide, 0.1 M glycolaldehyde, 0.25 M NaCN, and 0.5 M P_i was prepared in 10% D_2O at pH 7. A volume of 0.5 μL of dimethyl sulfoxide (DMSO) was added as a standard, and the ^{1}H NMR spectrum was recorded (initial solution). Next, the solution was dried down under reduced pressure at 30 °C and redissolved in 10% D_2O. The mixture was then heated at 50 °C and monitored over time by ^{1}H NMR spectroscopy. Two more dry–wet cycles were carried out in a similar manner for a total of three cycles. The intensities of the spectral regions containing 2-aminooxazole and the glycolaldehyde resonances were increased 10-fold for clarity. (*C*) A plot of the concentration versus time of glycolaldehyde and 2-aminooxazole determined by integration of the ^{1}H NMR data shown in *B* against DMSO for the three dry–wet cycles.

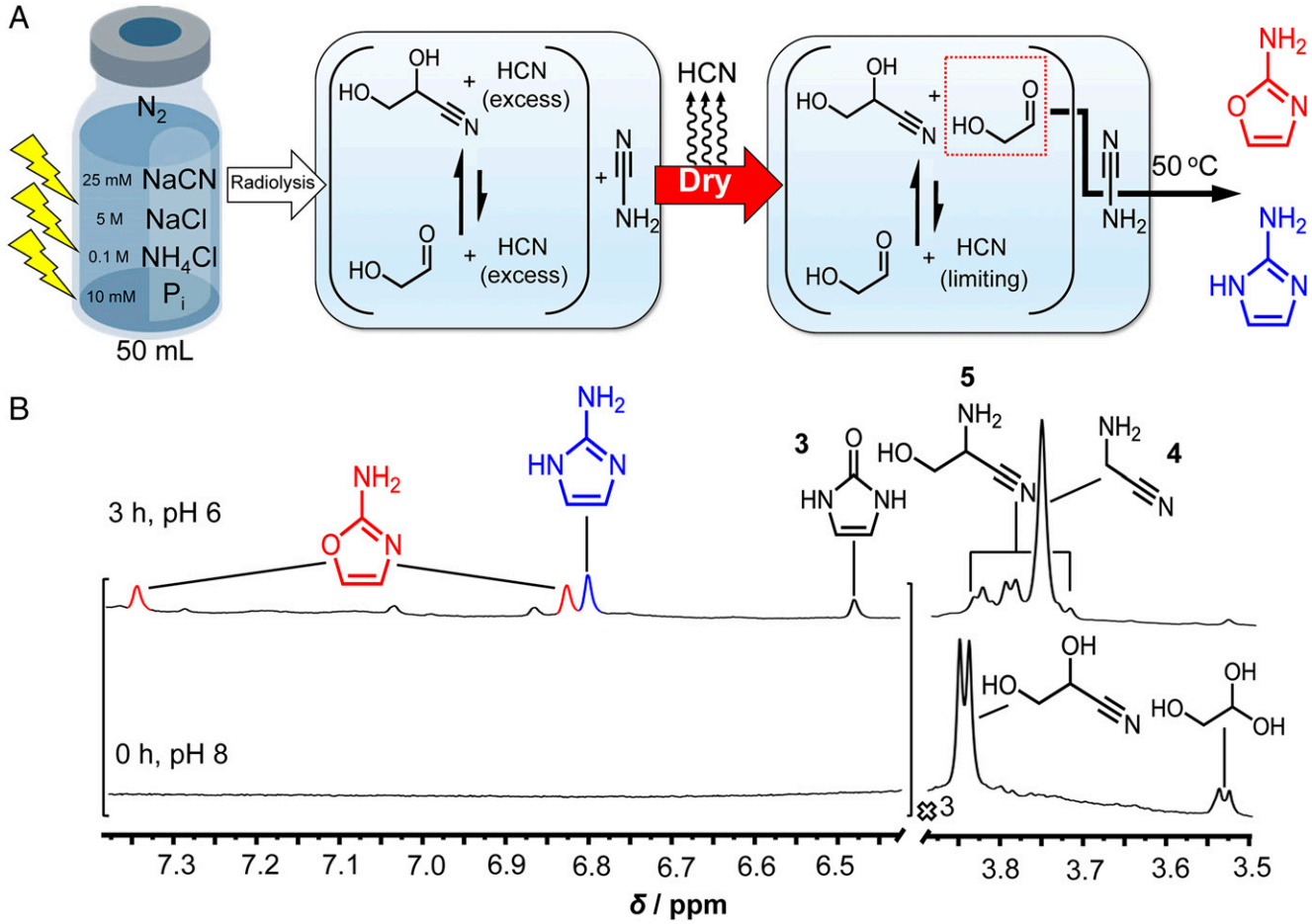

Fig. 2. (*A*) Scheme for the synthesis of 2-aminooxazole and 2-aminoimidazole from HCN by combining radiolysis with dry-down. A 50-mL solution of 25 mM NaCN, 0.1 M NH_4Cl, 5 M NaCl, and 10 mM P_i was prepared at pH 7 under an N_2 atmosphere, and exposed to γ radiation for ∼1 d (∼2.2 kGy·h^{-1}; total dose, ∼48 kGy) at ∼24 °C. Radiolysis results in the production of cyanamide and the glycolaldehyde-derived glyceronitrile in the presence of excess HCN. Following exposure (*SI Appendix*, Fig. S17), this solution was concentrated to ∼5 mL under reduced pressure at 35 °C. After drying, 450 μL of solution was transferred to an NMR tube along with 50 μL of D_2O, and the pH was adjusted to 8 (*SI Appendix*, Fig. S18). The solution in the tube was heated to 50 °C. After 3 h, the pH was adjusted to 6 in order to better resolve the 2-aminooxazole and 2-aminoimidazole resonances (*SI Appendix*, Fig. S19). (*B*) ^{1}H NMR data before and after heating for 3 h. The resonances were assigned by addition of standards.

a yield of 0.13% based on initial NaCN. The presence of free glycolaldehyde is consistent with the results shown in Fig. 1 that a portion of glyceronitrile is converted to free glycolaldehyde by removal of excess HCN during dry-down.

The concentrated irradiated solution was then heated at 50 °C, and monitored by ^{1}H NMR spectroscopy. After heating for 3 h, the ^{1}H NMR spectrum (Fig. 2*B*, *Top* trace, and *SI Appendix*, Figs. S3 and S19) reveals a pair of new resonances in the aromatic region that are assigned to 2-aminooxazole, while the glycolaldehyde signal is no longer detected. A new resonance assigned to 2-aminoimidazole is also observed. A singlet belonging to the constitutional isomer of 2-aminooxazole, namely 1,3-dihydro-2*H*-imidazol-2-one **3**, was also identified in the aromatic region of the spectrum. Quadrupole time-of-flight liquid chromatography mass spectrometry (Q-ToF-LCMS) analysis (*SI Appendix*, Fig. S28) of this mixture corroborates the production of 2-aminooxazole, 2-aminoimidazole, and 1,3-dihydro-2*H*-imidazol-2-one. Experimental evidence supporting a possible pathway for the production of compound **3** is shown in *SI Appendix*, Figs. S23 and S24, and does not involve glycolaldehyde or cyanamide, but 1-(cyanomethyl)urea. The concentrations of 2-aminooxazole and 2-aminoimidazole were determined to be ∼0.11 and ∼0.055 mM, respectively, which correspond to yields of 0.13% and 0.066% based on initial NaCN input. On the other hand, assuming that free glycolaldehyde obtained after dry-down is the limiting reagent, then these concentrations represent percent yields of 69% and 34% (approximately quantitative yield in total). These high yields can be attributed at least in part to the fact that the yields (and rates of formation) dramatically increase when large excesses of cyanamide to glycolaldehyde are employed (*SI Appendix*, Figs. S1, S4, and S5). Note that the concentration of cyanamide (2.8 mM) is in almost 20-fold excess over that of glycolaldehyde. Large absolute concentrations are also not required (*SI Appendix*, Fig. S7). Other mechanisms made possible by this complex mixture that do not rely on free glycolaldehyde obtained after dry-down may also contribute to the yields (see Table 1 for a summary of yields). Keeping the pH at 7 still furnishes 2-aminooxazole, albeit in a lower yield, favoring (26) more 2-aminoimidazole instead (*SI Appendix*, Fig. S20). The rate of 2-aminooxazole production (*SI Appendix*, Fig. S6) is decreased in NaCl solutions, but not so much as to inhibit the reaction. As a consequence of the large concentrations of NH_4^+/NH_3 present after dry-down, the remaining glycolonitrile and glyceronitrile are largely equilibrated to their amine analogs, namely, aminoacetonitrile **4** (39) and serinenitrile **5** (40), respectively, following this 3-h period of heating.

Table 1. Concentrations, synthetic yields (%), and radiolytic yields (*G*) of the compounds relevant to 2-aminooxazole and 2-aminoimidazole synthesis

Compound	Concentration, mM	Yield,* %	*G*
Cyanamide†	0.65	2.6	0.13
Glyceronitrile†	0.10	1.2	$2.0 \bullet 10^{-2}$
Cyanamide‡	2.8	1.1	$5.7 \bullet 10^{-2}$
Glyceronitrile‡	0.57	0.68	$1.1 \bullet 10^{-2}$
Glycolaldehyde‡	0.16	0.13	$3.3 \bullet 10^{-3}$
2-Aminooxazole§	$9.0 \bullet 10^{-2}$¶	0.11	$1.8 \bullet 10^{-3}$
2-Aminoimidazole§	$5.5 \bullet 10^{-2}$	$6.6 \bullet 10^{-2}$	$1.1 \bullet 10^{-3}$

All values were determined by ^{1}H NMR integration against an internal standard of DMSO, except for the case of cyanamide, which was quantified by HPLC analysis after derivatization with dansyl chloride.

*The yields are based on the initial amount of NaCN.

†Concentrations measured in the irradiated sample before dry-down (*SI Appendix*, Fig. S17).

‡Concentrations measured after dry-down resulting in a ∼10-fold decrease in volume (*SI Appendix*, Fig. S18).

§Concentrations measured after heating the sample following dry-down for 3 h at 50 °C (*SI Appendix*, Fig. S19).

¶The average concentration of 2-aminooxazole determined from two separate experiments.

Addition of Excess NaCN after Dry-Down Inhibits 2-Aminooxazole and 2-Aminoimidazole Production. A control experiment (*SI Appendix*, Fig. S21) was carried out whereby following dry-down, excess NaCN (enough to make a 0.1 M solution) was added back into the irradiated mixture. This addition resulted in the conversion of all of the free glycolaldehyde to glyceronitrile as observed by ^{1}H NMR spectroscopy. After 3 h of heating, no 2-aminooxazole or 2-aminoimidazole were detected.

2-Aminooxazole and 2-Aminoimidazole Are Not Observed When NaCl Is Omitted from the Initial Mixture. A control experiment omitting NaCl in the irradiated mixture was also carried out under otherwise the same conditions. After radiolysis, no cyanamide was detected (*SI Appendix*, Fig. S10) and no 2-aminooxazole or 2-aminoimidazole were observed by ^{1}H NMR spectroscopy after heating to 50 °C for 3 h following dry-down (*SI Appendix*, Fig. S22). These experiments confirm that NaCl is essential for the synthesis of 2-aminooxazole and 2-aminoimidazole in this reaction network.

Large Concentrations of P_i Diminish Radiolytic Yields of Cyanamide and Glyceronitrile. Control experiments using mixtures of pure reagents revealed that increasing the concentration of P_i (*SI Appendix*, Fig. S2) moderately increases the rate of 2-aminooxazole synthesis given low concentrations of glycolaldehyde and cyanamide. Large P_i concentrations (greater than ∼0.1 M) during radiolysis, however, were observed to hinder glyceronitrile and cyanamide production from aqueous mixtures of HCN (*SI Appendix*, Fig. S14). For these reasons, smaller concentrations of P_i are needed during radiolysis, while larger concentrations enhance subsequent synthesis. It was determined that 10 mM P_i initially included in the radiolysis mixture, once concentrated after dry-down, is sufficiently able to catalyze 2-aminooxazole production. Larger initial concentrations of P_i are not required nor actually benefit the overall synthesis. Caveats aside, it is clear that a separate well-timed addition step of P_i after radiolysis is not required.

Radiolysis of Glyceronitrile Yields the Cyanohydrin of Glyceraldehyde. D-Glyceraldehyde is the next intermediate needed in the Powner–Sutherland pathway, which reacts with 2-aminooxazole to produce (11) a mixture of 2-aminooxazoline stereoisomers. Radiolysis of aqueous glyceronitrile with a small excess of NaCN yields the cyanohydrin derivative of glyceraldehyde, i.e., 2,3,4-trihydroxybutanenitrile, as the major product observed by ^{1}H NMR spectroscopy (*SI Appendix*, Fig. S25). These experiments support the hypothesis that multiple cycles of radiolysis, dry-down, and replenishment of the HCN starting material can potentially lead to 2,3,4-trihydroxybutanenitrile accumulation. Furthermore, NMR spectroscopy and LCMS reveal that performing a dry–wet cycle on a mixture of 2-aminooxazole, glyceraldehyde, excess NaCN, and P_i buffer enables the synthesis of 2-aminooxazolines (*SI Appendix*, Figs. S27 and S29).

2-Aminooxazole Survives Radiolytic Exposure. The ability of 2-aminooxazole to survive radiolysis is required if it is to react with glyceraldehyde obtained by multiple cycles of radiolysis and dry-down. It was found that the concentration of 2-aminooxazole only decreased by about half following radiolysis under the same conditions employed for its production from HCN (*SI Appendix*, Fig. S26). For comparison, UV-photolysis of 2-aminooxazole under plausible solar-UV fluxes (210–290 nm) capable of reaching the surface of the early Earth yields (41) a half-life of 6.9 h.

Discussion

Radiolysis, when combined with dry-down, can effectively generate a reaction network that affords glycolaldehyde, cyanamide, 2-aminooxazole, and 2-aminoimidazole among a complex mixture of other compounds in a continuous manner. The inventory of radiolytic sources of energy present in the solar system, without taking into account relative intensities, include solar-derived UV photolysis (34, 42), charged particles emitted during solar flare events (24, 43), charged particles entrained along planetary magnetic field lines (44, 45), radioactive minerals in the crust (33, 46, 47), and galactic cosmic radiation (48). While the dose rates employed herein represent the upper limits of any of these radiolytic sources, high dose rates lessen the experimental time frames to more practical levels. The effect of lower dose rates requires further study and will enable the development of quantitative geochemical models that could help predict reaction network outcomes on long timescales that are experimentally impractical.

Dry-down cycles model hypothetical prebiotic geological environments where bodies of water transiently evaporate, such as riverbanks, puddles, salt pans, and coastlines, and may be rewetted in a (semi)periodic fashion. Such models have been shown to be effective for the nonenzymatic polymerization of biomonomers (49–52). The high concentrations of NaCl used here also are consistent with dry-down models. Geochemically realistic aqueous reservoirs are bound to contain some amount of chloride salts, which would tend to accumulate to saturation levels during evaporation. Indeed, it would be more difficult to argue for the absence of chloride salts than to assume their presence. Aqueous solutions containing NH_4Cl and NaCl have also been reported to facilitate (53) oligomerization of ribonucleotides when dried down. An additional benefit of dry-down is the increase in concentration of cyanamide, glycolaldehyde, and phosphate present in the irradiated mixtures. Although the yields of 2-aminooxazole and 2-aminoimidazole based on initial NaCN are only a fraction of a percent, the yields based on available glycolaldehyde are essentially quantitative even in the presence of this complex mixture. We hypothesize a similar network of reactions will occur if the initial mixture were allowed to undergo slow evaporation while being irradiated, but testing this hypothesis is outside our current experimental capabilities. Nevertheless, there likely exists a range of evaporation and irradiation dose rates that can generate 2-aminooxazole and 2-aminoimidazole in yields comparable to those reported here.

The simplified radiolytic reaction network showing only those compounds relevant to 2-aminooxazole and 2-aminoimidazole synthesis is shown in Fig. 3, and all other identified compounds in this radiolytic network are shown in Fig. 4. Additional proposed mechanisms of compounds are shown in Fig. 4 and *SI Appendix*, Schemes. The proposed network is driven largely by

the redox power generated from briny water radiolysis. At high NaCl concentrations, direct ionization (54) of chloride along with water is also possible, yielding ·Cl as well as a significant fraction of the total e^-_{aq} production (55). Additional pathways reported for ·Cl mediated by reaction of Cl^- with H_3O^+ or ·OH are reproduced in *SI Appendix*. The intermediate organic radicals are not explicitly shown in Fig. 3 for the sake of clarity; likewise, multiple pathways leading to the same compounds may exist but are not represented here.

The energy of a single ^{60}Co γ-ray photon (on the order of 1 MeV) is vastly greater than any covalent bond (in the range of 1 to 20 eV). Therefore, the supposition that γ irradiation will act indiscriminately leading to a random distribution of products across the theoretical space of possible organic structures is not unreasonable. This outcome, however, is not observed, and instead, only a small set of organic species is identified as major products. This result may be explained by the fact that, despite the overwhelming energy of the γ photon, the ensuing chemistry primarily arises from the redox power of e^-_{aq}/·H, ·OH, and ·Cl, species that are achieved after the energy of the γ photon has been dissipated to thermal levels (56). The energy of the γ ray is thus "funneled down" into these fundamental radical species, which is proposed to drive much of the resulting chemistry. In fact, the oxazolidinone **8** identified herein was also observed as one of the end products after UV-photolysis of cyanocuprates in the presence of excess HCN (36). Despite the many order-of-magnitude difference in energy between γ and UV photons, a similar reaction network is observed. Calvin also noted that exposing atmospheric mixtures to different sources of energy tended to produce a common set of compounds: "What is obtained in the first approximation depends more upon the composition of the starting material than it does on the nature of the energy input" (57). Regardless of whether continuous radiolytic reaction networks played a direct role in the origins of life, they can nonetheless provide insights into the possible compounds that may have been sampled from the vast library of organic structure space (58).

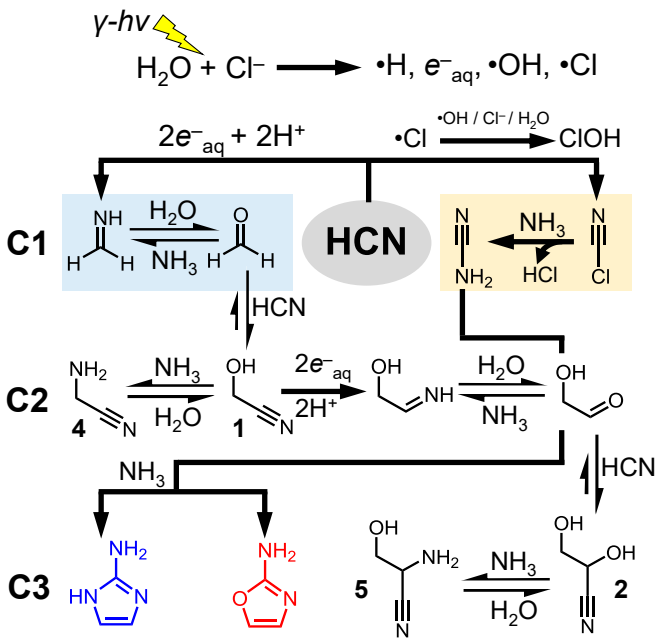

Fig. 3. Simplified reaction network showing the pathways relevant to 2-aminooxazole and 2-aminoimidazole synthesis achieved from the radiolysis of HCN followed by dry-down. Organic radical intermediates have not been explicitly shown for clarity. For further details of the proposed radiolytic radical mechanisms, see *SI Appendix*, Schemes.

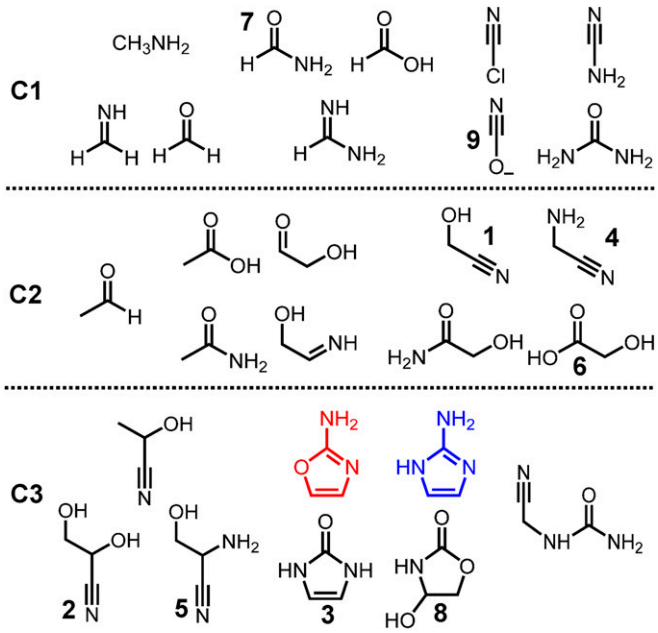

Fig. 4. The compounds identified in the radiolytic reaction network. All compounds shown were either identified by addition of commercially acquired and synthesized standards, or otherwise inferred. Methanimine, formaldehyde, acetaldehyde, and 2-iminoethanol are inferred by the observation of aminoacetonitrile, glycolonitrile, lactonitrile, and serinenitrile, respectively, while glycolaldehyde is inferred from the direct NMR detection of its gem-diol form. Cyanogen chloride was observed in previously reported (35) radiolysis experiments under similar high NaCl concentrations. For further details of the proposed mechanisms, see *SI Appendix*, Schemes.

Identifying all of the products formed and their interconnecting pathways is crucial for understanding the overall behavior of the reaction network, especially in response to changing conditions. Understanding these synthetic relationships could aid in the discovery of possible emergent features, properties that cannot be detected in discontinuous synthetic models or which otherwise limit the production of complex mixtures. Radiolytic reaction pathways for many of the C1 compounds in Fig. 4 have been studied previously (4, 59–63). While accounting for all of the reaction pathways connecting these polar compounds with each other is beyond the scope of the present study, a few should be noted for context. For example, aminoacetonitrile **4** and serinenitrile **5** are direct precursors to glycine and serine, respectively, via nitrile hydrolysis (64). Glycolic acid **6** has been reported to act as a catalyst for the condensation of amino acids driven ultimately by a dry-down step (49), as well as a precursor to long oligomers in its own right (51). The C1 compound formamide **7** is often cited as an alternative solvent to water, which, in neat form, facilitates a variety of different condensation processes (47, 65). The 1,3-dihydro-2*H*-imidazol-2-one **3** has been employed as an alternative nucleobase (66) toward the construction of an expanded genetic code. All of these species arising in the same mixture suggests a means of studying how nucleic and amino acid precursors might coevolve.

Conclusions

In summary, 2-aminooxazole, an intermediate in the Powner–Sutherland pathway, is generated from a continuous reaction network starting from HCN as the only carbon feedstock. The structurally similar 2-aminoimidazole, a compound useful for nonenzymatic template-directed RNA synthesis, is also produced. The progression of chemical reactions in this network is driven by the combination of γ radiolysis with dry-down. After

radiolysis, dry-down removes excess HCN from the mixture, shifting the equilibrium away from glyceronitrile, and generating the free glycolaldehyde that can be exploited for 2-aminooxazole and 2-aminoimidazole synthesis. The synthesis of these compounds is still achieved under relatively low concentrations of glycolaldehyde and cyanamide, as well as in the presence of a variety of other organics that are also produced. The reaction network proceeds with only minimal interference from the experimenter, i.e., no intermediary purification steps or well-timed additions of reagents/catalysts are required. Although the yield based on the amount of initial NaCN of any one compound in the network may be low, such yields are unavoidable in order to generate a complex mixture of compounds from a single organic starting material. Complex mixtures of this type have been called (67) the "prebiotic chemist's nightmare," but this sentiment may be shared by the chemistry community as a whole—the tendency to avoid (68) complexity in many chemical disciplines is prevalent. Embracing complexity (68), nevertheless, may be the remedy needed to wake us from the nightmare into the "molecular biologist's dream" (67). For example, the Krishnamurthy laboratory (69) showed recently that nonenzymatic RNA replication rather than being hindered in fact benefits from greater complexity in the form of heterogeneous chimeric templates. Future work will focus on mapping out reaction pathways for other chemical members of the reaction network, and testing whether further cycles of radiolysis followed by dry-down can generate the next set of higher-order aminooxazoline products related to the Powner–Sutherland pathway in a continuous fashion.

Materials and Methods

For general methods, γ-radiolysis procedures, high-performance liquid chromatography (HPLC), NMR spectroscopy, LCMS, and additional schemes, see *SI Appendix*.

Data Availability. All of the necessary data can be found in *SI Appendix*.

ACKNOWLEDGMENTS. This work was supported in part by Japan Society for the Promotion of Science KAKENHI Grant-in-Aid for Scientific Research on Innovative Areas "Hadean Bioscience," Grant JP26106003, and by the World Premier International Research Center-funded Earth-Life Science Institute at the Tokyo Institute of Technology. Thanks to the Earth-Life Science Institute's Research Interactions Committee for travel funding. This work was supported by a grant from the Simons Foundation (494291) (to Z.R.A.). We acknowledge the support of the Australian Nuclear Science and Technology Organisation and the Tokyo Institute of Technology for providing the ^{60}Co gamma radiolysis facilities used in this work. We acknowledge the help of the NMR Facility within the Mark Wainwright Analytical Centre at the University of New South Wales and the Strategic Hires and Retention Pathways (SHARP) for financial support.

1. A. Lazcano, "Complexity, self-organization and the origin of life: The happy liaison?" in *Origins of Life Self-Organization and/or Biological Evolution*, (EDP Sciences, Paris, 2009), pp. 13–22.
2. P. Nghe *et al*., Prebiotic network evolution: Six key parameters. *Mol. Biosyst.* **11**, 3206–3217 (2015).
3. S. L. Miller, H. C. Urey, Organic compound synthesis on the primitive earth. *Science* **130**, 245–251 (1959).
4. M. Ruiz-Bermejo, M.-P. Zorzano, S. Osuna-Esteban, Simple organics and biomonomers identified in HCN polymers: An overview. *Life (Basel)* **3**, 421–448 (2013).
5. K. B. Muchowska, S. J. Varma, J. Moran, Synthesis and breakdown of universal metabolic precursors promoted by iron. *Nature* **569**, 104–107 (2019).
6. R. Shapiro, Prebiotic ribose synthesis: A critical analysis. *Orig. Life Evol. Biosph.* **18**, 71–85 (1988).
7. H. J. Cleaves II, The prebiotic geochemistry of formaldehyde. *Precambrian Res.* **164**, 111–118 (2008).
8. H.-J. Kim *et al*., Synthesis of carbohydrates in mineral-guided prebiotic cycles. *J. Am. Chem. Soc.* **133**, 9457–9468 (2011).
9. R. F. Gesteland, T. R. Cech, J. F. Atkins, Eds., *The RNA World: The Nature of Modern RNA Suggests a Prebiotic RNA World*, (Cold Spring Harbor Laboratory Press, ed. 3, 2006).
10. R. A. Sanchez, L. E. Orgel, Studies in prebiotic synthesis. V. Synthesis and photoanomerization of pyrimidine nucleosides. *J. Mol. Biol.* **47**, 531–543 (1970).
11. M. W. Powner, B. Gerland, J. D. Sutherland, Synthesis of activated pyrimidine ribonucleotides in prebiotically plausible conditions. *Nature* **459**, 239–242 (2009).
12. S. Becker *et al*., A high-yielding, strictly regioselective prebiotic purine nucleoside formation pathway. *Science* **352**, 833–836 (2016).
13. S. Stairs *et al*., Divergent prebiotic synthesis of pyrimidine and 8-oxo-purine ribonucleotides. *Nat. Commun.* **8**, 15270 (2017).
14. A. Biscans, Exploring the emergence of RNA nucleosides and nucleotides on the early Earth. *Life (Basel)* **8**, 57 (2018).
15. N. Kitadai, S. Maruyama, Origins of building blocks of life: A review. *Geoscience Frontiers* **9**, 1117–1153 (2018).
16. S. Becker *et al*., Unified prebiotically plausible synthesis of pyrimidine and purine RNA ribonucleotides. *Science* **366**, 76–82 (2019).
17. R. Shapiro, The improbability of prebiotic nucleic acid synthesis. *Orig. Life* **14**, 565–570 (1984).
18. R. Shapiro, Small molecule interactions were central to the origin of life. *Q. Rev. Biol.* **81**, 105–125 (2006).
19. S. A. Benner, H.-J. Kim, M. A. Carrigan, Asphalt, water, and the prebiotic synthesis of ribose, ribonucleosides, and RNA. *Acc. Chem. Res.* **45**, 2025–2034 (2012).
20. J. Tour, Animadversions of a synthetic chemist. *Inference Int. Rev. Sci.* **2**, 2 (2016).
21. C. Richert, Prebiotic chemistry and human intervention. *Nat. Commun.* **9**, 5177 (2018).
22. H. J. Cleaves II, Prebiotic chemistry: What we know, what we don't. *Evol. Educ. Outreach* **5**, 342–360 (2012).
23. K. Kurosawa *et al*., Hydrogen cyanide production due to mid-size impacts in a redox-neutral N_2-rich atmosphere. *Orig. Life Evol. Biosph.* **43**, 221–245 (2013).
24. V. S. Airapetian, A. Glocer, G. Gronoff, E. Hébrard, W. Danchi, Prebiotic chemistry and atmospheric warming of early Earth by an active young Sun. *Nat. Geosci.* **9**, 452–455 (2016).
25. C. Anastasi, M. A. Crowe, M. W. Powner, J. D. Sutherland, Direct assembly of nucleoside precursors from two- and three-carbon units. *Angew. Chem. Int. Ed. Engl.* **45**, 6176–6179 (2006).
26. A. C. Fahrenbach *et al*., Common and potentially prebiotic origin for precursors of nucleotide synthesis and activation. *J. Am. Chem. Soc.* **139**, 8780–8783 (2017).
27. L. Li *et al*., Enhanced nonenzymatic RNA copying with 2-aminoimidazole activated nucleotides. *J. Am. Chem. Soc.* **139**, 1810–1813 (2017).
28. D. J. Ritson, C. Battilocchio, S. V. Ley, J. D. Sutherland, Mimicking the surface and prebiotic chemistry of early Earth using flow chemistry. *Nat. Commun.* **9**, 1821 (2018).
29. D. Whitaker, M. W. Powner, Prebiotic nucleic acids need space to grow. *Nat. Commun.* **9**, 5172 (2018).
30. M. Calvin, The Bakerian Lecture, 1965—chemical evolution. *Proc. R. Soc. Lond. A* **288**, 441–466 (1965).
31. I. G. Draganić, Radiolysis of water: A look at its origin and occurrence in the nature. *Radiat. Phys. Chem.* **72**, 181–186 (2005).
32. I. Draganić, *The Radiation Chemistry of Water*, (Academic Press, 1971).
33. T. Ebisuzaki, S. Maruyama, Nuclear geyser model of the origin of life: Driving force to promote the synthesis of building blocks of life. *Geoscience Frontiers* **8**, 275–298 (2017).
34. S. Ranjan, D. D. Sasselov, Influence of the UV environment on the synthesis of prebiotic molecules. *Astrobiology* **16**, 68–88 (2016).
35. R. Yi, Y. Hongo, I. Yoda, Z. R. Adam, A. C. Fahrenbach, Radiolytic synthesis of cyanogen chloride, cyanamide and simple sugar precursors. *ChemistrySelect* **3**, 10169–10174 (2018).
36. D. Ritson, J. D. Sutherland, Prebiotic synthesis of simple sugars by photoredox systems chemistry. *Nat. Chem.* **4**, 895–899 (2012).
37. J. Xu *et al*., Photochemical reductive homologation of hydrogen cyanide using sulfite and ferrocyanide. *Chem. Commun. (Camb.)* **54**, 5566–5569 (2018).
38. M. W. Powner, S.-L. Zheng, J. W. Szostak, Multicomponent assembly of proposed DNA precursors in water. *J. Am. Chem. Soc.* **134**, 13889–13895 (2012).
39. G. Moutou *et al*., Equilibrium of α-aminoacetonitrile formation from formaldehyde, hydrogen cyanide and ammonia in aqueous solution: Industrial and prebiotic significance. *J. Phys. Org. Chem.* **8**, 721–730 (1995).
40. S. Islam, D.-K. Bučar, M. W. Powner, Prebiotic selection and assembly of proteinogenic amino acids and natural nucleotides from complex mixtures. *Nat. Chem.* **9**, 584–589 (2017).
41. Z. R. Todd, R. Szabla, J. W. Szostak, D. D. Sasselov, UV photostability of three 2-aminoazoles with key roles in prebiotic chemistry on the early earth. *Chem. Commun. (Camb.)* **55**, 10388–10391 (2019).
42. V. M. Canuto, J. S. Levine, T. R. Augustsson, C. L. Imhoff, M. S. Giampapa, The young Sun and the atmosphere and photochemistry of the early Earth. *Nature* **305**, 281–286 (1983).
43. D. S. Smith, J. Scalo, J. C. Wheeler, Transport of ionizing radiation in terrestrial-like exoplanet atmospheres. *Icarus* **171**, 229–253 (2004).
44. A. H. Armstrong, F. B. Harrison, H. H. Heckman, L. Rosen, Charged particles in the inner Van Allen radiation belt. *J. Geophys. Res.* **66**, 351–357 (1961).
45. C. F. Chyba, C. B. Phillips, Europa as an abode of life. *Orig. Life Evol. Biosph.* **32**, 47–68 (2002).
46. J. Parnell, Mineral radioactivity in sands as a mechanism for fixation of organic carbon on the early Earth. *Orig. Life Evol. Biosph.* **34**, 533–547 (2004).
47. Z. R. Adam *et al*., Estimating the capacity for production of formamide by radioactive minerals on the prebiotic Earth. *Sci. Rep.* **8**, 265 (2018).
48. U. R. Rao, Solar modulation of galactic cosmic radiation. *Space Sci. Rev.* **12**, 719–809 (1972).

49. J. G. Forsythe *et al*., Ester-mediated amide bond formation driven by wet–dry cycles: A possible path to polypeptides on the prebiotic earth. *Angew. Chem. Int. Ed. Engl.* **54**, 9871–9875 (2015).
50. D. S. Ross, D. Deamer, Dry/wet cycling and the thermodynamics and kinetics of prebiotic polymer synthesis. *Life (Basel)* **6**, 28 (2016).
51. K. Chandru *et al*., Simple prebiotic synthesis of high diversity dynamic combinatorial polyester libraries. *Nat. Commun.* **1**, 30 (2018).
52. I. Mamajanov, Wet-dry cycling delays the gelation of hyperbranched polyesters: Implications to the origin of life. *Life (Basel)* **9**, 56 (2019).
53. L. Da Silva, M.-C. Maurel, D. Deamer, Salt-promoted synthesis of RNA-like molecules in simulated hydrothermal conditions. *J. Mol. Evol.* **80**, 86–97 (2015).
54. A. Balcerzyk *et al*., Picosecond pulse radiolysis of direct and indirect radiolytic effects in highly concentrated halide aqueous solutions. *J. Phys. Chem. A* **115**, 9151–9159 (2011).
55. A. K. El Omar, U. Schmidhammer, B. Rousseau, J. LaVerne, M. Mostafavi, Competition reactions of $H_2O^{\bullet+}$ radical in concentrated Cl^- aqueous solutions: Picosecond pulse radiolysis study. *J. Phys. Chem. A* **116**, 11509–11518 (2012).
56. Z. Adam, A. C. Fahrenbach, S. M. Jacobson, B. Kacar, D. Y. Zubarev, Radiolysis generates a complex organosynthetic chemical network. ChemRxiv:10.26434/chemrxiv.10148684.v1 (13 November 2019).
57. M. Calvin, "Primitive (prebiotic) chemistry" in *Chemical Evolution: Molecular Evolution Towards the Origin of Living Systems on the Earth and Elsewhere*, (Oxford University Press, 1969), pp. 121–143.
58. M. Meringer, H. J. Cleaves, Exploring astrobiology using *in silico* molecular structure generation. *Philos. Trans. Royal Soc. Math. Phys. Eng. Sci.* **375**, 20160344 (2017).
59. H. Büchler, R. E. Bühler, R. Cooper, Pulse radiolysis of aqueous cyanide solutions. Kinetics of the transient OH and H adducts and subsequent rearrangements. *J. Phys. Chem.* **80**, 1549–1553 (1976).
60. B. H. J. Bielski, A. O. Allen, Radiation chemistry of aqueous cyanide ion. *J. Am. Chem. Soc.* **99**, 5931–5934 (1977).
61. Z. D. Draganić, V. Niketić, S. Jovanović, I. G. Draganić, The radiolysis of aqueous ammonium cyanide: Compounds of interest to chemical evolution studies. *J. Mol. Evol.* **15**, 239–260 (1980).
62. J. C. Aponte *et al*., Pathways to meteoritic glycine and methylamine. *ACS Earth Space Chem.* **1**, 3–13 (2017).
63. A. Sato *et al*., First-principles study of the formation of glycine-producing radicals from common interstellar species. *Mol. Astrophys.* **10**, 11–19 (2018).
64. S. L. Miller, J. E. Van Trump, "The Strecker synthesis in the primitive ocean" in *Origin of Life*, Y. Wolman, Ed. (Springer, 1981), pp. 135–141.
65. R. Saladino, G. Botta, S. Pino, G. Costanzo, E. Di Mauro, Genetics first or metabolism first? The formamide clue. *Chem. Soc. Rev.* **41**, 5526–5565 (2012).
66. I. Hirao *et al*., A two-unnatural-base-pair system toward the expansion of the genetic code. *J. Am. Chem. Soc.* **126**, 13298–13305 (2004).
67. G. F. Joyce, L. E. Orgel, "Prospects for understanding the origin of the RNA world" in *The RNA World*, R. F. Gesteland, J. F. Atkins, Eds. (Cold Spring Harbor Laboratory Press, ed. 1, 1993), pp. 1–25.
68. J. F. Stoddart, Editorial: From supramolecular to systems chemistry: Complexity emerging out of simplicity. *Angew. Chem. Int. Ed. Engl.* **51**, 12902–12903 (2012).
69. S. Bhowmik, R. Krishnamurthy, The role of sugar-backbone heterogeneity and chimeras in the simultaneous emergence of RNA and DNA. *Nat. Chem.* **11**, 1009–1018 (2019).